AIP | Journal of Applied Physics

Magnetic anisotropy and stacking faults in Co and Co84Pt16 epitaxially grown thin films

Vincent Sokalski, David E. Laughlin, and Jian-Gang Zhu

Citation: J. Appl. Phys. **110**, 093919 (2011); doi: 10.1063/1.3658861
View online: http://dx.doi.org/10.1063/1.3658861
View Table of Contents: http://jap.aip.org/resource/1/JAPIAU/v110/i9
Published by the American Institute of Physics.

Magnetic anisotropy and stacking faults in Co and $Co_{84}Pt_{16}$ epitaxially grown thin films

Vincent Sokalski,[1,a)] David E. Laughlin,[1,b)] and Jian-Gang Zhu[2,c)]
[1]*Material Science & Engineering, Data Storage Systems Center, Carnegie Mellon University, Pittsburgh, Pennsylvania 15213, USA*
[2]*Electrical & Computer Engineering, Data Storage Systems Center, Carnegie Mellon University, Pittsburgh, Pennsylvania 15213, USA*

(Received 9 August 2011; accepted 27 September 2011; published online 11 November 2011)

A combined set of experimental and theoretical diffraction studies are performed to evaluate the possible impact of stacking faults on magnetic anisotropy using epitaxially grown Co/Ru and $Co_{84}Pt_{16}$/Ru thin films on MgO(111) single crystal substrates. A 3rd nearest neighbor interaction is incorporated into Monte Carlo simulations of faulted film growth used to predict (10.L) diffraction profiles. These are compared with experimental profiles to determine stacking fault content. It is found that stacking fault density decreases with increasing temperature concurrent with an increase in magnetic anisotropy and a compression of the crystallographic lattice parameter, c. © *2011 American Institute of Physics*. [doi:10.1063/1.3658861]

I. INTRODUCTION

Reduction of noise in perpendicular magnetic recording (PMR) media is critical to improving areal recording density beyond 1 Tbit/in^2. Noise can occur due to thermal instability of magnetic bits or a wide grain-to-grain switching field distribution, which is likely to arise due to non-uniformity in the media microstructure.[1–3] The recording layer of today's media is comprised of, at least, two hexagonal close-packed (HCP) CoPt-based layers: a granular layer having CoPt grains segregated by oxide grain boundaries and a capping layer that is continuous and serves to provide uniform intergranular exchange coupling.[4] These layers are grown on an HCP Ru(00.1) underlayer, which serves as a template to transfer HCP stacking to the CoPt layers, induce strong (00.1) texture, and reduce grain size. Stacking faults in HCP Co-alloy media have been previously studied for their potentially detrimental effect on media performance.[5,6] It is believed that local breaking of the uniaxial symmetry due to stacking faults will reduce magnetic anisotropy, K_u, causing thermal instability and reduced switching field. A stacking fault in the HCP structure creates a layer of atoms that are in a face-centered cubic (FCC) environment that is, magnetically, more isotropic. The variance of the number of defects in a grain (e.g., impurities, vacancies, dislocations, or stacking faults) scales with the square root of its expected value. Stacking faults are a planar defect and tend to span an entire layer within a grain. As grains in media have only ~ 50 atomic layers, the variation in the number of stacking faults among grains will be substantial for any finite stacking fault probability.

Quantitatively measuring stacking fault density in real media by XRD is quite difficult, due to the weak diffracted intensity from the fiber-textured grains for geometries other than out-of-plane $\theta/2\theta$ scans. High resolution TEM analyses are often not statistically significant, and sample preparation may alter stacking fault content. Furthermore, separating the effect of stacking faults on magnetic properties from other extrinsic parameters in media is very challenging. Here, we use epitaxially grown Co-based films on MgO(111) single crystal substrates to minimize other extrinsic factors (e.g., grain size, chemical segregation, interface effects) that might affect magnetic anisotropy while also allowing for more quantitative evaluation of stacking fault content by XRD.

II. EXPERIMENTAL PROCEDURES

A series of 15-nm Co or $Co_{84}Pt_{16}$(00.1) thin films are grown by RF sputtering with varying growth temperature (25–368 °C) on MgO(111) single crystal substrates with a 15-nm Ru(00.1) buffer layer grown at 500 °C. The argon working pressure was fixed at 5 mTorr with a base pressure maintained at better than 2×10^{-7} Torr. Films were sputtered from a pure Co and a $Co_{84}Pt_{16}$ alloy target. Deposition rates were calibrated by step profilometry, and thicknesses were verified by cross-section TEM.

Magnetic measurements were performed using a Princeton Measurements alternating gradient field magnetometer (AGFM). K_{perp} was determined from the area between in-plane and perpendicular M-H loops and was used to calculate magnetic anisotropy by $K_u = K_{perp} + 2\pi M_s^2$. K_{perp} is defined as positive for a perpendicular easy axis and negative for an in-plane easy axis.

Stacking faults were evaluated by XRD measurements using a Phillips X'Pert Pro diffractometer. Reciprocal space q-scans were performed to give the Co or $Co_{84}Pt_{16}$(10.L) profile. It is well established that stacking faults cause certain reciprocal lattice spots to broaden along the (00.1)* direction.[7,8] Specifically, indices having H-K = 3 N, where N is an integer, will be unaffected by stacking faults, while all others are broadened with the extent of broadening, depending on the parity of L. Note that capital (HKL) notation is

[a)]Electronic mail: vsokalsk@andrew.cmu.edu.
[b)]Electronic mail: laughlin@cmu.edu.
[c)]Electronic mail: jzhu@ece.cmu.edu.

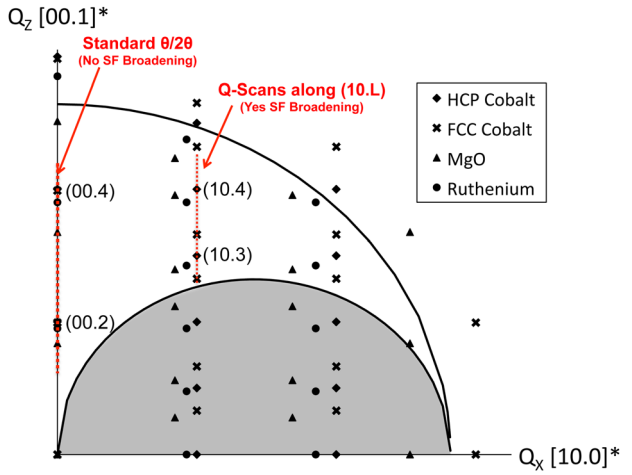

FIG. 1. (Color online) Schematic reciprocal space map showing possible key diffraction spots for HCP and FCC cobalt as well as HCP Ru and MgO. Dashed lines indicate where measurements were performed to evaluate stacking fault content. The gray shaded region is only accessible by tilting the film normal out of the scattering plane.

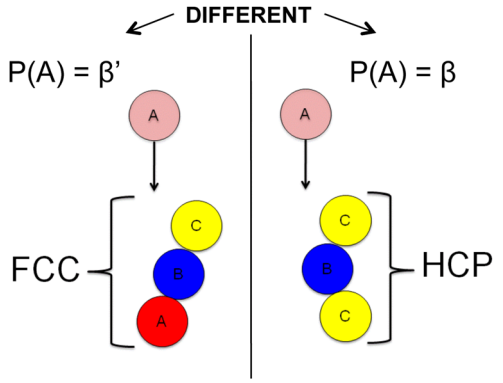

FIG. 2. (Color online) Suggested growth model incorporating 3rd nearest neighbor interactions. β and β' are the probabilities that a new atomic layer has a different lateral position than that which is two layers beneath it (i.e., a growth fault). β applies when the previous 3 layers are in an ABA-type of stacking sequence, while β' applies when the previous 3 layers are in an ABC-type of stacking sequence.

commonly used to avoid confusion with the continuous reciprocal space variables, h_1, h_2, and h_3. The widths of all peaks were determined by fitting to the pseudo-Voigt function.[9,10] Broadening due to stacking faults was determined by comparing the width of the (10.3) and (10.4) peaks, which should broaden, due to stacking faults, with the (00.4) peak, which should not broaden, as shown in Fig. 1. These peaks were selected so that the film normal does not need to be rotated out of the scattering plane, which can cause excess broadening when using a line-focused beam, as is the case here. The effects of stacking faults on diffraction are determined from Monte Carlo simulations and used to interpret experimental observations. Changes in lattice parameter, c, were determined from the position of the (00.4) peaks in a $\theta/2\theta$ scan. The epitaxial relationship was verified by XRD $\theta/2\theta$ and φ-scans.

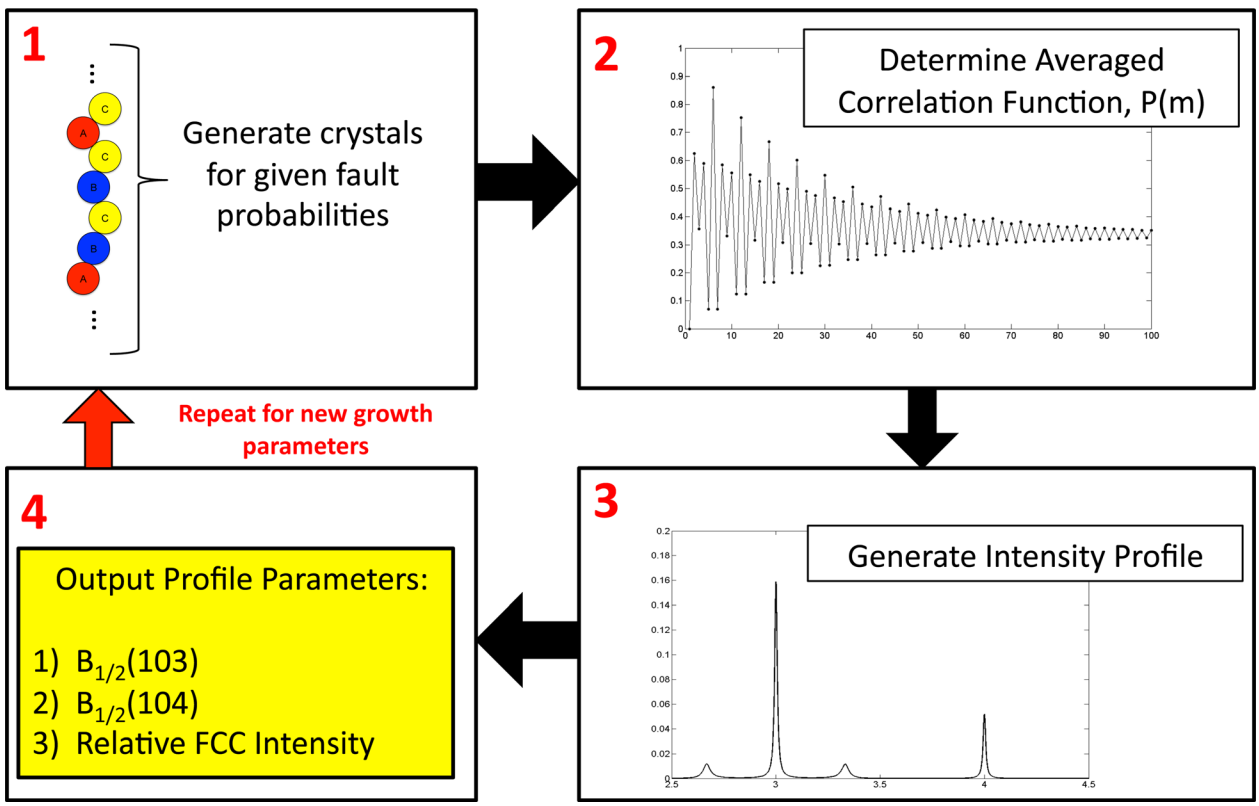

FIG. 3. (Color online) Monte Carlo simulation flow chart used to determine the effect of fault probabilities on the (10.L) diffraction profile. 1D crystals were generated for a given set of stacking fault probabilities, from which an average correlation function, P(m), was determined and used to generate a theoretical (10.L) diffraction profile. The peak widths and relative FCC/HCP peak intensities were determined from these simulated profiles.

III. SIMULATIONS

In order to improve our interpretation of experimental broadening results, Monte Carlo simulations have been performed to predict the extent of broadening due to non-randomly distributed stacking faults. The diffracted intensity for a close-packed structure with N layers is given by[11,12]

$$I = \sum_{m=1}^{N-1} (N-m)\left\{P_m^0 + (1-P_m^0)cos[2\pi(H-K)/3]\right\}cos(m\pi h_3). \quad (1)$$

Here, h_3 is a continuous variable along the c* reciprocal lattice direction, H and K are the first two Miller indices in hexagonal coordinates, and P_m^0 is a correlation function describing the probability of two close packed planes that are m layers apart having the same lateral position (e.g., both planes are an "A"). $P(1) = 0$ for all cases, as two neighboring planes never have the same stacking position, while $P(\infty) = 1/3$ as long as there is a finite stacking fault probability.

Analytical solutions for P_m^0 in a faulted HCP crystal have been derived for many cases, including the cases of randomly distributed growth faults, where a single layer is in an FCC environment (e.g., ABABCBCB), and/or deformation faults, where two neighboring layers are in an FCC environment (e.g., ABABCACA).[7,8,13] The assumption that a material is comprised of only growth and deformation faults is often made, because each of these fault types has a reasonable mechanism for its formation. This assumption also leads to an elegant solution for the amount of broadening due to stacking faults. Nonetheless, for the case of thin films, the formation of stacking faults should be dominated by the growth mechanism (i.e., each layer of deposited material either grows with the correct or incorrect stacking sequence). Here, we suggest that the probability of a new layer growing with the correct HCP stacking position is determined by the stacking sequence of the previous three layers. This is described by two probabilities, β and β', as shown schematically in Fig. 2. Such a description is equivalent to saying that, once a crystal begins growing with FCC stacking, subsequent layers have a higher than normal chance to continue to grow with FCC stacking. A similar description was originally proposed by Jagodzinski and solved analytically.[14] β can be thought of as the number of stacking faults in a crystal, while β' is related to the average size of the faults (i.e., how many layers a fault spans). This description also does not restrict the system to only two possible types of stacking faults.

Four thousand crystals with 1000 layers were "grown" in Monte Carlo simulations for varying fault probabilities, β and β' (see Fig. 3). The correlation function was determined for all crystals and averaged before inputting into Eq. (1) to produce a plot of the (10.L) intensity profile. Three parameters can be determined from the calculated intensity profile, $B_{\frac{1}{2}}$ (10.3), $B_{\frac{1}{2}}$ (10.4), and the relative intensity at possible FCC peaks, which occur on either side of (10.3) peak displaced by 1/3. These are the same values that can be measured experimentally from XRD q-scans. It should be noted that the result would be the same for any pair of (10.L) peaks as long as one peak had L = odd and the other L = even.

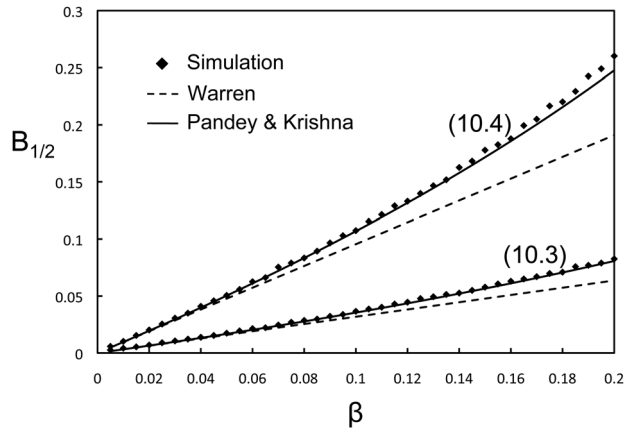

FIG. 4. Monte Carlo diffraction simulations for the case of randomly distributed growth faults (i.e., $\beta = \beta'$), showing the dependence of peak width on fault probability, β. The simulations are compared with analytical solutions according to Warren and Pandey and Krishna, as indicated.

In order to verify the accuracy of the simulation, our results were compared to the original equations from Warren[8]

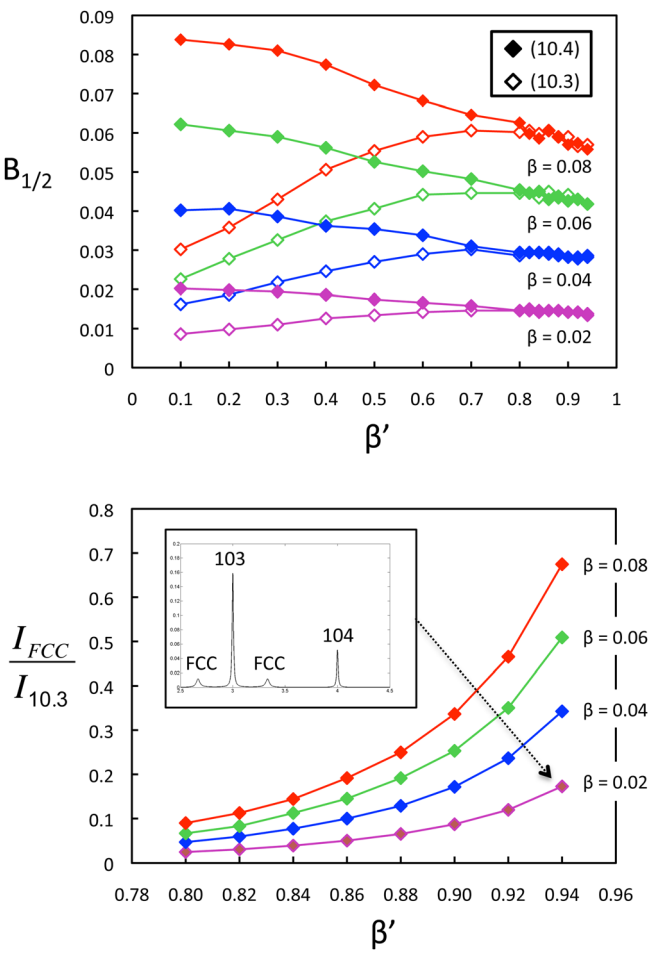

FIG. 5. (Color online) Monte Carlo simulation results showing the dependence of peak width (top) and relative FCC intensity (bottom) on β'. The inset is an example simulated profile for $\beta' = 0.94$ and $\beta = 0.02$.

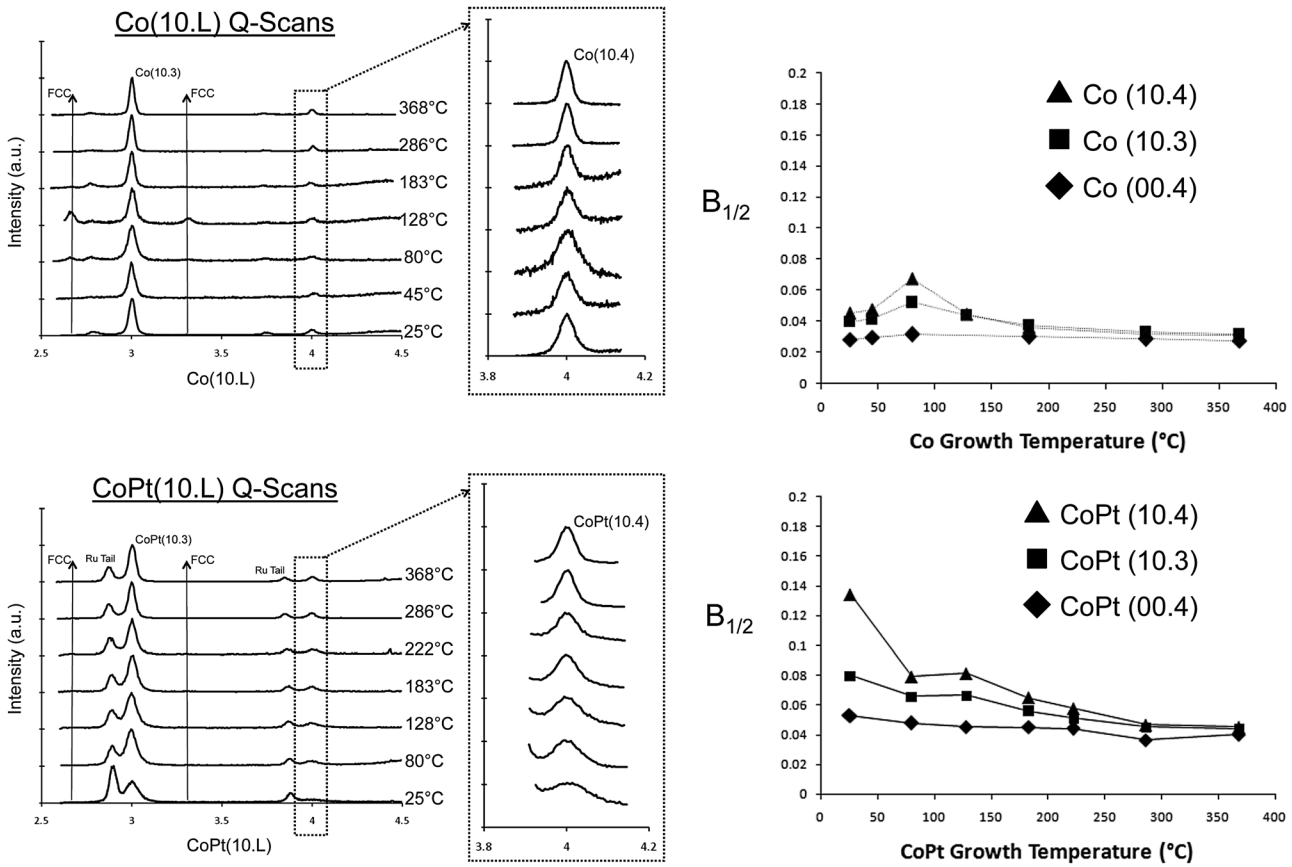

FIG. 6. Left Experimentally measured (10.L) Q-scans for Co (top) and $Co_{84}Pt_{16}$ (bottom). The temperatures indicated on the plot are the growth temperatures of Co or $Co_{84}Pt_{16}$. Right: Experimentally measured (10.3), (10.4), and (00.4) peak widths for Co (top) and $Co_{84}Pt_{16}$ (bottom) as a function of Co or $Co_{84}Pt_{16}$ growth temperature.

as well as to the more general solution based on Pandey and Krishna[15,16] for randomly distributed growth faults (Fig. 4). The effect of β' on the peak width and relative FCC intensity for fixed β is shown in Fig. 5. Increasing β' causes $B_{\frac{1}{2}}$ (10.4)/$B_{\frac{1}{2}}$ (10.3) to decrease from 3 (for $\beta' = 0$) to 1(for $\beta' > 0.7$). It is only for very large values of β' (~ 0.8) that the FCC intensity becomes significant.

IV. RESULTS AND DISCUSSION

(10.L) q-scans with corresponding peak width measurements are shown in Fig. 6 for Co and $Co_{84}Pt_{16}$. The appearance of Ru peaks just prior to $Co_{84}Pt_{16}$ is due to the close lattice spacing of Ru and $Co_{84}Pt_{16}$, but do not affect the measured peak widths. The width of the (00.4) peaks remain relatively constant, with no measurable change for the case of Co and a slight decrease in width for increasing growth temperature in $Co_{84}Pt_{16}$ films. No FCC peaks were observed in $Co_{84}Pt_{16}$ for any growth temperature. For the Co film grown at 128 °C, small FCC peaks were observed ($I_{FCC}/I_{(10.3)} = 0.25$), indicating a large value of β'. Broadening of the Co and $Co_{84}Pt_{16}$ (10.L) peaks can be interpreted as follows, based on the simulations: In both cases, β is less than 1.5% for growth temperatures above 150 °C. Below 150 °C, Co tends to grow with a lower density of stacking faults than $Co_{84}Pt_{16}$, but with a larger average size.

The same measurements were made for the Ru underlayer (Fig. 7), which is known to have a very high stacking fault energy, to ensure consistency in the experiments. It was observed that the width of all three Ru peaks are roughly equal, indicating that the broadening seen for Co and $Co_{84}Pt_{16}$ is not instrumental.

M-H loops for $Co_{84}Pt_{16}$ are shown in Fig. 8, with complete K_u versus temperature data in Fig. 9. For both cases, the magnetic anisotropy increases with temperature. The $Co_{84}Pt_{16}$ easy axis switches from in-plane to perpendicular

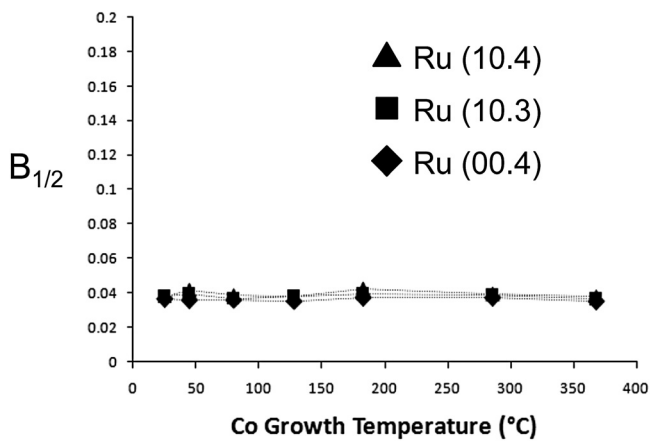

FIG. 7. Experimentally measured Ru(10.3), Ru(10.4), and Ru(00.4) peak widths for Co(15 nm)/Ru(15 nm)/MgO(substrate) films as a function of Co growth temperature. The Ru growth temperature was fixed at 500 °C.

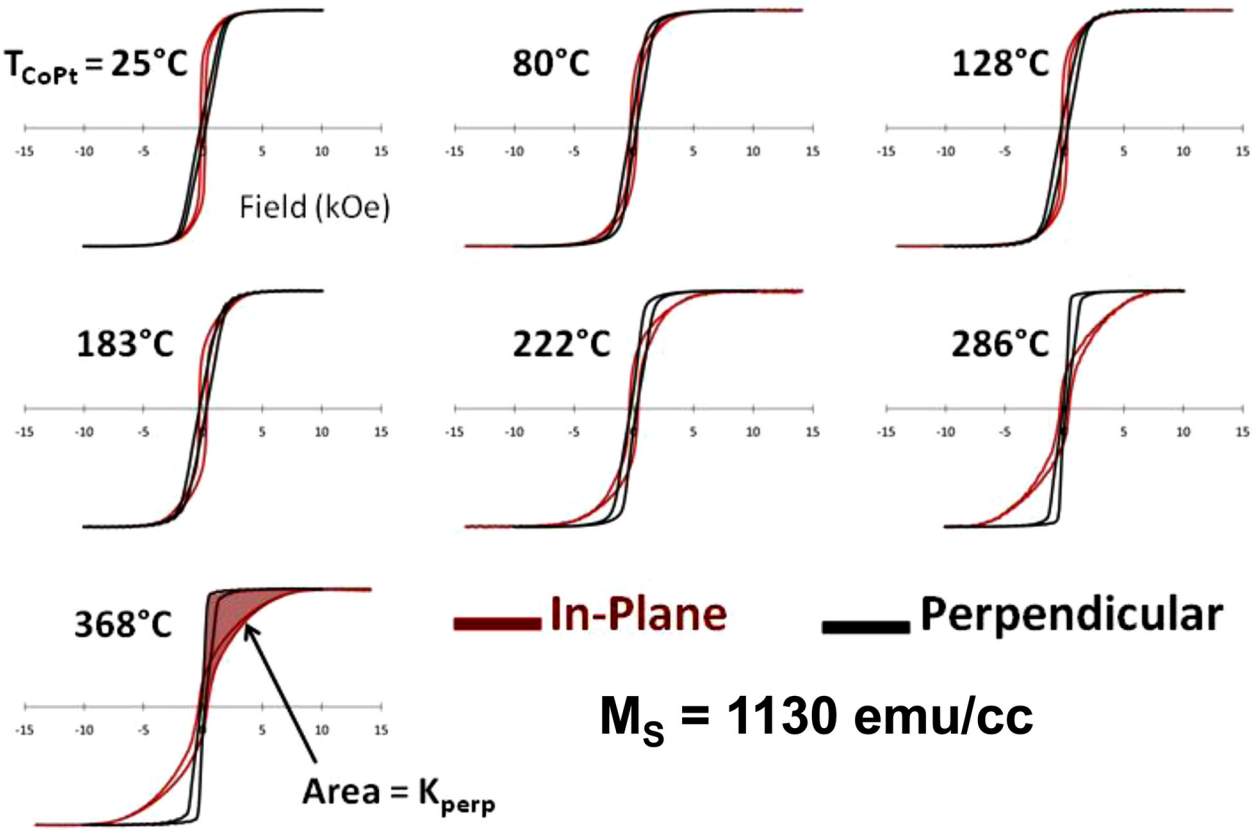

FIG. 8. (Color online) Measured M-H loops for $Co_{84}Pt_{16}$(15 nm)/Ru(15 nm)/MgO films. The temperatures indicated in the figure are the growth temperatures for the $Co_{84}Pt_{16}$ layer.

above 200 °C, while the easy axis always remains in-plane for pure Co, due to the larger M_s and smaller K_u. Similar trends have been observed in the past for $Co_{84}Pt_{16}$ alloys and were attributed to long-range chemical ordering with alternating Co and Pt close-packed planes to form either an ordered HCP derivative structure[17,18] or the $L1_1$ FCC derivative structure.[19] Superlattice reflections were not observed in any $Co_{84}Pt_{16}$ films prepared in this work, indicating that chemical ordering is absent or, at least, very limited.

The observation of a lower stacking fault density at higher temperature could be explained by thermally activated self-healing. The HCP to FCC transition temperature in cobalt occurs at 420 °C, with HCP being the stable phase at lower temperature. Therefore, it is reasonable to believe that the further below this transition temperature a system is, the stronger the driving force will be to eliminate stacking faults (i.e., FCC layers). Even though the driving force may be higher, sufficient surface atom mobility is needed for the assimilation of an FCC region by an HCP region. Busse *et al.*[20] have proposed several mechanisms for the healing of stacking faults, which are suggested to become active at critical temperatures, which were calculated for the case of FCC iridium. The activation of such a mechanism in the range of 150–200 °C could explain the temperature dependence seen here for stacking fault probability and K_u.

Correlations between K_u, β, and HCP lattice parameter (c) are shown in Fig. 10. It is important to note that it is the growth fault probability, β, which is being shown, and the possible influence of β' cannot be determined from these figures. The most compelling correlation is the strong linear trend observed for K_u versus c. Such a trend has been reported previously in the literature[21,22] and is qualitatively consistent with bulk measurements of magnetostriction for single crystal cobalt, where a compression

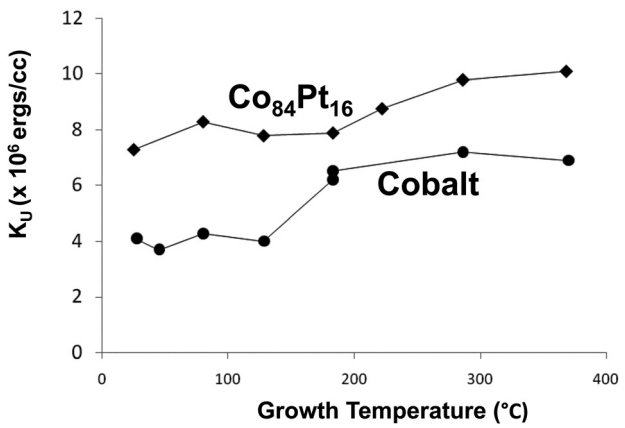

FIG. 9. Dependence of magnetocrystalline anisotropy, K_u, on Co-alloy growth temperature for Co and $Co_{84}Pt_{16}$ thin films.

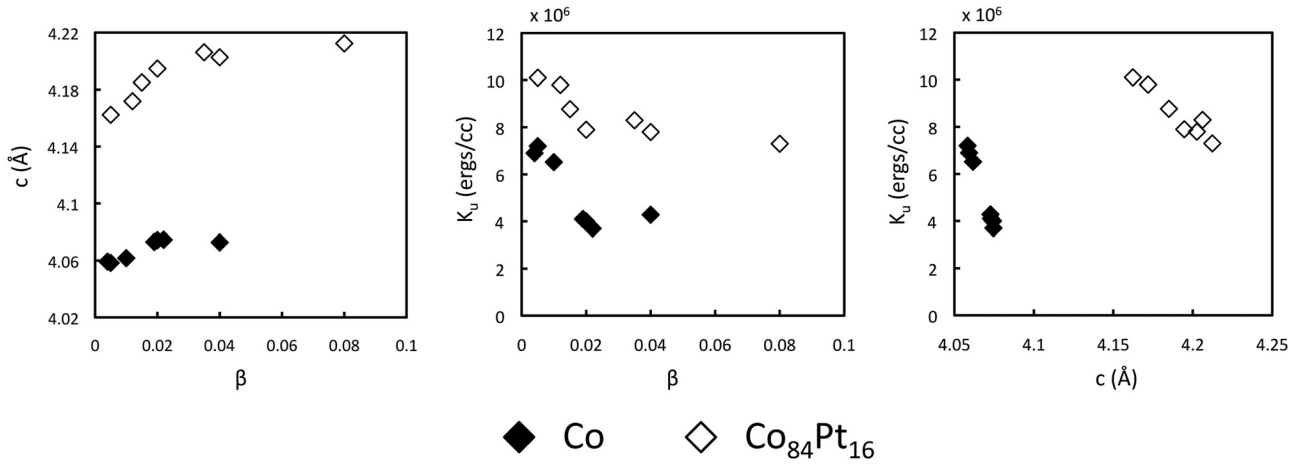

FIG. 10. Experimentally determined correlations between magnetic anisotropy (K_u), growth fault probability (β), and HCP lattice parameter (c) in Co and $Co_{84}Pt_{16}$ thin films.

of the c-axis increases magnetic anisotropy.[23] The data shown is also consistent with expected correlations for c vs. β and K_u vs. β. Because $d_{111,FCC} > d_{00.2,HCP}$ in Co,[24] it is reasonable to expect an increase in close packed plane spacing for higher stacking fault densities. However, the non-linear dependence on β does not have a clear physical explanation, which may indicate that the controlling factor is the lattice parameter, c. Stacking faults could have an indirect effect on magnetic anisotropy via their influence on the crystallographic lattice parameter, which may overshadow the more obvious effect of breaking the uniaxial HCP symmetry. Another possible factor affecting the lattice parameter is unrelieved strain from the larger HCP Ru underlayer, which cannot be distinguished from the effect of stacking faults on lattice parameter at this point.

V. CONCLUSION

The possible impact of stacking faults on the magnetic anisotropy of Co and $Co_{84}Pt_{16}$ films was studied by combination of XRD measurements and Monte Carlo simulations. A 3rd nearest neighbor interaction is implemented in the simulations to improve our interpretation of peak broadening. We conclude that the stacking fault content decreases with increasing growth temperature for both Co and $Co_{84}Pt_{16}$, likely due to thermally activated healing. At lower temperature, Co tends to grow with a lower density of faults as compared to $Co_{84}Pt_{16}$, but with a larger average size. In both cases, the magnetic anisotropy has a strong linear correlation to the lattice parameter, c. We suggest that unrelieved strain from the Ru underlayer as well as a change in plane spacing due to stacking faults may contribute to the measured variations in lattice parameter. The results here highlight the importance of crystal structure uniformity throughout perpendicular magnetic recording media in addition to the well-recognized need for a uniform microstructure.

ACKNOWLEDGMENTS

The authors would like to thank Showa Denko (SDK) and the Data Storage Systems Center (DSSC) of Carnegie Mellon University for financial support.

[1]J.-G. Zhu, V. Sokalski, Y. Wang, and D. Laughlin, IEEE Trans. Magn. **47**, 7 (2011).
[2]S. N. Piramanayagam and K. Srinivasan, J. Magn. Magn. Mater. **321**, 485 (2009).
[3]L. Pu-Ling and S. H. Charap, IEEE Trans. Magn. **30**, 4230 (1994).
[4]G. Choe, M. Zheng, B. R. Acharya, E. N. Abarra, and J. N. Zhou, IEEE Trans. Magn. **41**, 3172 (2005).
[5]B. Lu, T. Klemmer, K. Wierman, G. Ju, D. Weller, A. Roy, D. E. Laughlin, C. Chang, and R. Ranjan, J. Appl. Phys. **91**, 3 (2002).
[6]S. Saito, A. Hashimoto, D. Hasegawa, and M. Takahashi, J. Phys. D: Appl. Phys. **42**, 7 (2009).
[7]A. Wilson, Proc. R. Soc. London, Ser. A **180**, 277 (1942).
[8]B. E. Warren, Prog. Met. Phys. **8**, 56 (1959).
[9]M. Birkholz, *Thin Film Analysis by X-ray Scattering* (Wiley VCH, Berlin, 2006).
[10]G. K. Wertheim, M. A. Butler, K. W. West, and D. N. E. Buchanan, Rev. Sci. Instrum. **45**, 1369 (1974).
[11]S. Shrestha and D. Pandey, Europhys. Lett. **34**, 269 (1996).
[12]P. Tiwary and D. Pandey, Acta Crystallogr. **63**, (2007).
[13]J. W. Christian, Acta Crystallogr. **7**, 2 (1954).
[14]V. Jagodzinski, Acta Crystallogr. **2**, 208 (1949).
[15]D. Pandey and P. Krishna, J. Phys. D: Appl. Phys. **10**, 2057 (1977).
[16]M. T. Sebastian and P. Krishna, *Random, Non-Random, and Periodic Faulting in Crystals* (Gordon and Breach, New York, 1994).
[17]G. R. Harp, D. Weller, T. Rabedeau, R. Farrow, and M. Toney, Phys. Rev. Lett. **71**, 2493 (1993).
[18]Y. Yamada, T. Suzuki, H. Kanazawa, and J. Osterman, J. Appl. Phys. **85**, 5094 (1999).
[19]H. Sato, T. Shimatsu, Y. Okazaki, H. Muraoka, and H. Aoi, J. Appl. Phys. **103**, 3 (2008).
[20]C. Busse and T. Michely, Surf. Sci. **552**, 13 (2004).
[21]T. Shimatsu, H. Sato, Y. Okazaki, H. Aoi, H. Muraoka, and Y. Nakamura, J. Appl. Phys. **99**, 08G908-1 (2006).
[22]J.-J. Wang, T. Sakurai, K. Oikawa, K. Ishida, N. Kikuchi, S. Okamoto, H. Sato, T. Shimatsu, and O. Kitakami, J. Phys: Condens. Matter **21**, 185008 (2009).
[23]R. C. O'Handley, *Modern Magnetic Materials: Principles and Applications* (Wiley, New York, 2000).
[24]B. D. Cullity and S. R. Stock, *Elements of X-ray Diffraction*, 3rd ed. (Prentice-Hall, Englewood Cliffs, NJ, 2001).